ACS OMEGA

Open Access

http://pubs.acs.org/journal/acsodf

Article

Experimental Study on the Preparation of Lignin-Based Activated Carbon and the Adsorption Performance for Phenol

Ping Cao, Yuting Li,* and Jingli Shao

Cite This: *ACS Omega* 2024, 9, 24453−24463

Read Online

ACCESS | Metrics & More | Article Recommendations

ABSTRACT: Biomass waste and wastewater are important wastes in the process of industrialization, which need to be effectively treated and utilized. In this work, an innovative method of collaborative treatment of biomass waste and phenol-containing wastewater is proposed. Biomass waste was used to produce activated carbon (AC), and then AC was used for phenol removal in wastewater treatment. Two kinds of typical biomass waste material, namely, coconut shell and lignin, were used. Physical activation (steam activation) and chemical activation methods were compared. Results show that steam activation is an effective method for coconut shell AC production. The largest Brunauer−Emmett−Teller (BET) surface area was 1065 m^2/g at 800 °C. Chemical activation could produce AC samples with higher BET specific surface area. The lignin AC with K_2CO_3 activation has the largest BET surface of 1723.8 m^2/g at 800 °C. FTIR results indicated that K_2CO_3 activation could greatly enhance the formation of surface oxygen-containing functional groups. Both coconut shell AC and lignin AC samples show excellent performance for phenol removal. The highest phenol removal efficiency for coconut shell AC and lignin AC are 96.87% and 98.22%, respectively. Adsorption kinetic analysis show that the pseudo-first-order kinetic model is able to describe the adsorption characteristics of phenol in wastewater treatment. Recycling properties show that regeneration of lignin AC could maintain high adsorption performance for phenol.

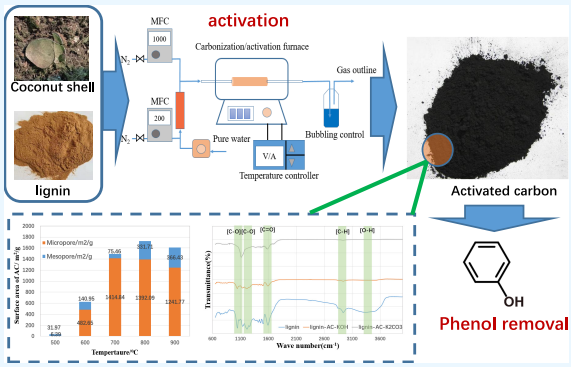

1. INTRODUCTION

With the development of industry, the discharge of wastewater has increased sharply, bringing increasing water pollution problems.[1] Phenol and its derivatives are important raw materials for industrial resins, fuels, powders, coal chemicals, biofuels, and other industries.[2,3] The discharge of phenol-containing wastewater in the process of production and use of phenol will cause serious environmental pollution. An extended period of exposure to phenol may lead to abnormal breathing, tremor followed by coma, and respiratory arrest when reaching human lethal doses.[4] In an aquatic environment, there was significant proof that phenol affects growth of aquatic life. For instance, fish exposed to phenol wastewater have shown disrupted growth based on their reduced weight.[5] Therefore, how to treat phenolic wastewater with high efficiency and reduce environmental pollution is an urgent problem to be solved.[6]

The phenolic wastewater produced in the production process can be treated separately according to its concentration. For high-concentration phenol-containing wastewater, recycling can be adopted to recycle it.[6,7] For low-concentration phenol-containing wastewater, which cannot be recycled, it can be treated by physical, chemical, or biological methods to reduce its concentration to meet the discharge standard.[8] The physical method is the basic method of separation, recovery, or treatment of phenol-containing wastewater, and the common physical methods include adsorption, liquid membrane separation, and extraction. Among them, the adsorption method is the use of adsorbent developed pore structure, large specific surface area and pore capacity, surface functional groups and other characteristics, adsorption recovery, or removal of phenolic substances in water method.[9,10] Adsorption methods can be divided into physical adsorption, chemical adsorption, etc. In principle, the adsorption of pollutants can be carried out through hydrogen bonding, van der Waals forces, and other forces.[11] When the adsorption material reaches saturation, it can be desorbed by alkali solution, organic solvent, or heating regeneration. Activated carbon, resin, graphene, molecular sieves, and other adsorbents are used for water treatment.[12,13]

Ahmad et al.[14] used phosphoric acid as an activator and biochar prepared from bamboo waste to treat printing and dyeing wastewater, and the specific surface area of the activated carbon prepared reached 988.23 m^2/g. The results showed that

Received: January 10, 2024
Revised: May 8, 2024
Accepted: May 14, 2024
Published: May 29, 2024

https://doi.org/10.1021/acsomega.4c00352
ACS Omega 2024, 9, 24453−24463

the removal rates of chroma and COD reached 91.84% and 75.21%. Patel et al.[15] used activated carbons prepared from sawdust, sugar cane bagasse, and pine needles to treat greywater. The sawdust activated carbon was found to be more efficient. Under the operating optimum conditions, the percentage removal of COD and BOD are found to be 97.83% and 95.83% for sawdust AC. Ferraz et al.[16] recycled oat hulls to produce activated carbon, which is chemically activated with phosphoric acid. The results showed that the activated carbon prepared by 100% phosphoric acid impregnation had a high specific surface area (1090−3880 m^2/g), and the decolorization rate and COD removal rate reached 100% and 90%, respectively. Khurshid et al.[17] used phosphoric acid and hydrogen peroxide solution to treat waste tea residue to prepare activated carbon, and the results showed that the combined modified activated carbon had more oxygen-containing functional groups and specific surface areas, and the maximum COD removal rate could reach 95.5%. These early practices and good performance have proven the feasibility of activated carbon in the field of wastewater treatment.

Carbonaceous materials come from a wide range of sources and have large specific surface areas, developed pore structure, and surface functional groups.[18] In terms of economics, carbonaceous materials can achieve efficient purification treatment of wastewater at a lower cost. Therefore, based on the above characteristics, carbonaceous functional materials are regarded as perfect wastewater treatment materials.[19] The preparation of activated carbon from solid waste and its application in the treatment of phenolic wastewater have the advantages of comprehensive utilization of waste. Therefore, the cooperative disposal of solid waste and phenolic wastewater could be achieved by the preparation of activated carbon.

The preparation of activated carbon mainly includes three steps: raw material selection, carbonization process, and activation process. Carbonization is the pyrolysis of raw materials to form a carbon structure. Activation is the most important step in the preparation of activated carbon. The activator is in contact with the microcrystalline structure of carbonaceous materials such as graphite fragments under high temperature conditions, so that it expands to produce a large number of nanomicroporous structures and improves the specific surface area and porosity of activated carbon. Recently, a one-step activation method for activated carbon production has also been gradually adopted, which directly mixes raw material with activator to produce activated carbon. With chemical activator is used, the surface functional groups can be modified and retained.[20]

Therefore, using waste biomass waste to produce activated carbon for wastewater treatment is a potential method for comprehensive utilization of biomass waste. Coconut shell is a typical forestry waste, which is largely produced in tropical regions. Naturally, the coconut shell waste is either left to rot or is directly used as burning fuel, which has an impact on the environment and is a waste of resources. Hence, the conversion of coconut shell solid waste into activated carbon, particularly the shell is most desirable.[21] Coconut shell activated carbon has the advantages of well-developed pores, good adsorption performance, high strength, and easy regeneration, is economic and durable, and is widely used in water treatment, decolorization, medicine, and other fields.[22] Lignin black liquor is the main waste in the paper industry.[23] It is generally known that black liquor is a kind of toxic and severely colored paper pulp sewage. Its dark coloration and toxicity can reduce oxygen availability and negatively affect water resources.[24] The recovery and utilization of lignin from black liquor is crucial. Dieste et al.[25] used black liquor as fuel to be burned in the recovery boiler, generating an excess of energy that was converted to electricity and sold to the grid. Fu et al.[26] used lignin as the raw material to prepare activated carbon via a two-step method. Zhao et al.[27] recently prepared porous carbon materials from black liquor lignin and utilized them as a CO_2 adsorbent. Exploring the preparation of high performance activated carbon from waste coconut shells and lignin for phenol adsorption and wastewater treatment is a research area with high economic value. At present, there is a lack of sufficient research in this field.

In this work, coconut shells and lignin were used as typical biomass waste to produce activated carbon samples. Two kinds of activation methods, namely, steam activation (two step method) and chemical activation (one step method), were used to produce activated carbon samples. The effect of temperature and activation methods on the properties of activated carbon was studied. The phenol adsorption performance over activated carbon samples was studied. In the end, kinetic analysis of the phenol adsorption on AC samples was conducted. This work provides a new approach for the collaborative treatment of biomass waste and phenol-containing wastewater.

2. EXPERIMENTAL SECTION

2.1. Materials. Coconut shell was collected from Hainan Province in China. The coconut shell was dried and crushed into powder with diameters ranging from 200 to 500 μm. Lignin was alkaline style (CAS: 8068-05-1) and was purchased from Sigma-Aldrich Corporation. The ultimate analysis of the samples was determined using an elemental analyzer (Elementar Vario EL). The composition of coconut shell and lignin was summarized in Table 1.

Table 1. Ultimate Analysis of Biomass Samples[a]

	Ultimate analysis (wt%)				
Sample	C	H	O	N	Ash
Coconut shell	48.92	5.28	0.46	44.52	0.82
Lignin	56.62	5.12	0.12	34.52	3.62

[a]Prior to the experiment, all samples were kept in a drying oven at a controlled temperature of 30 °C.

2.2. Preparation of Activated Carbon. The carbonization and activation experiments were carried out on a tubular furnace, as shown in Figure 1.

The furnace reactor was made of an alundum tube, with an inner diameter of 60 mm and a length of 750 mm. When heating,

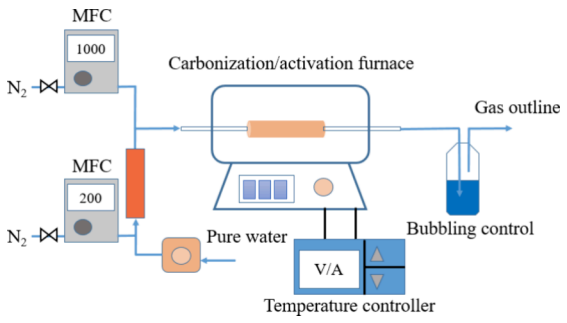

Figure 1. Experimental apparatus for activated carbon production.

https://doi.org/10.1021/acsomega.4c00352
ACS Omega 2024, 9, 24453−24463

the middle of the pipe was a constant temperature zone, and the length was about 200 mm, where the biomass or biochar samples were located for carbonization or activation. A program temperature control module was used to control the heating of the furnace and maintain the reaction temperature. During carbonization, the heating rate was controlled at 10 K/min and the final temperatures were set as 300, 400, 500, 600, and 700 °C. The activation of biochar was divided into two kinds: physical activation and chemical activation. During physical activation, the steam was used as the activation agent, which was controlled by the peristaltic pump, and then the water was heated by a steam evaporator. The activation temperature was first controlled at 700−900 °C, and then the sample was located in the furnace. The activation time could be varied from 30 to 120 min. During chemical activation, the about 3 g material was added to the K_2CO_3 or KOH solution and left for 2 h (the mass of K_2CO_3/KOH powder is twice that of coconut shell char or lignin powder) and dried in the oven at 105 °C for 24 h. The dry mixture was placed in a quartz boat, placed in a tube furnace, and activated in a nitrogen atmosphere for 40 min at an activation temperature of 800 °C. Then the activation product can be obtained by natural cooling to room temperature, and the resulting activation product is filtered and cleaned with ultrapure water until the filtrate is neutral. Finally, the samples were dried at 105 °C for 24 h to obtain lignin-based activated carbon samples.

In the adsorption kinetics experiment, 50 mL of phenol solution (100 mg/L) was taken each time, 0.2 g of different activated carbon samples were added to the solution, and the solution was stirred and adsorbed on a constant temperature magnetic agitator. Within 0−30 min, a solution sample was removed every 5 min, the absorbance of phenol in the solution was measured after the solid was filtered, and the concentration of phenol after adsorption was obtained according to the standard curve of phenol. The calculation formula of the adsorption rate at any time is

$$\eta(\%) = \frac{C_0 - C_t}{C_0} \times 100\% \quad (1)$$

in which η refers to the phenol adsorption efficiency at time of t, C_0 refers to the initial concentration of phenol (mg/L), and C_t refers to the concentration of phenol at time t.

The pseudo-first-order kinetic model and pseudo-second-order kinetic model are two typical adsorption kinetic models that are important for studying the diffusion process.[28,29] The kinetic parameter k could also be used to analyze the adsorption rate.

According to the pseudo-first-order kinetic model, the effect of reaction rate is mainly attributed to the resistance of molecular diffusion in the particle, and the difference between the adsorption amount Q_t and the equilibrium adsorption amount Q_e of the adsorbent at time t during the adsorption process is proportional to the adsorption amount of the adsorbent.

$$Q_t = Q_e(1 - e^{-kt}) \quad (2)$$

in which Q_t refers to the adsorption mass (mg/g) at time t, Q_e refers to the adsorption mass (mg/g) at the equilibrium state, and k refers to the adsorption rate constant (min^{-1}).

2.3. Analysis Method. The BET surface area, pore volume, and pore diameter of activated carbon samples were tested and analyzed using the N_2 adsorption−desoprtion isotherms obtained at −196 °C with an automatic instrument (TriStar II 3020, Micromertics). Prior to the adsorption test, all samples were degassing in a vacuum at 280 °C for 300 min. The specific surface area (S_{BET}) was determined by the Brunauer−Emmett−Teller (BET) method.[30,31] The total pore volume was calculated from the N_2 adsorption isotherm in the relative pressure range of 0−0.995. The micropore volume and external surface area (mesoporous surface area) were measured by the t-plot method. The average pore diameter was calculated from the N_2 adsorption isotherm by the Barrett−Joyner−Halenda (BJH) method.[32]

The functional groups of raw material and AC samples were analyzed by Bruker's Vertex 70 Fourier transform infrared (FTIR) spectrometer. A mixture of samples and KBr powder with a mass ratio of 1:100 was milled into a powder mixture, and then the mixture powder was sampled by compression under 15 MPa pressure. The compressed flake then was analyzed by FTIR. The settings of the FTIR instrument were as follows: Resolution was 2 cm^{-1}. Scanning frequency was 10 kHz. The wavenumber varied from 4000 to 650 cm^{-1}.

3. RESULTS AND DISCUSSION

3.1. Carbonization of Coconut Shell. As pointed out above, carbonization is the first step during traditional two-step activation of carbon production. The initial structural characteristics of pyrolysis char itself have a significant impact on subsequent physical activation. Therefore, the carbonization of coconut shell was first studied.

The influence of temperature on the yield of pyrolysis char was summarized in Figure 2.

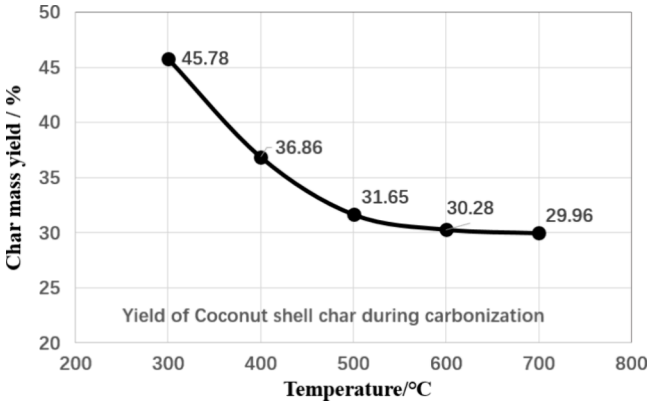

Figure 2. Biochar yield of coconut shell at different temperature.

It can be seen that the yield of coconut shell char decreased with the pyrolysis temperature. At low temperature (300 °C), the yield of char is 45.78 wt %, which is due to the release of surface moisture, dehydration reaction, and initial decomposition of cellulose, hemicellulose, and lignin.[33] When the temperature increased to 400 °C, the char yield quickly decreased to 36.86 wt %, which was attributed to the extensive decomposition of cellulose and lignin.[34,35] When the temperature further increased to 500 °C, the char yield decreased to about 31.65 wt % and was maintained at relative stability at higher temperatures. It can be seen that at 500 °C there is still some volatile compound retained in the char. The lattice structure of char does not show graphitization or inertness, which is conducive to the subsequent physical activation process of pore formation. Therefore, 500 °C could be chosen as the

https://doi.org/10.1021/acsomega.4c00352
ACS Omega 2024, 9, 24453−24463

carbonization temperature for coconut shell during the two-step activation carbon production. Wei et al.[36] also reached a similar conclusion.

3.2. Steam Activation of Coconut Shell Char. Next, steam activation of coconut shell char was conducted. Steam is a kind of typical activation agent during physical activation.[36] The heterogeneous reaction between char and steam (gasification reaction) was controlled by reaction temperature, residence time, and the amount of steam.[37] In the optimized condition, part of the carbon element in the char matrix was consumed and the retained char was called activated carbon, which is rich in a large number of microscopic pores.[38] The influence of activation temperature on the activated carbon yield and BET specific surface area was summarized in Figure 3.

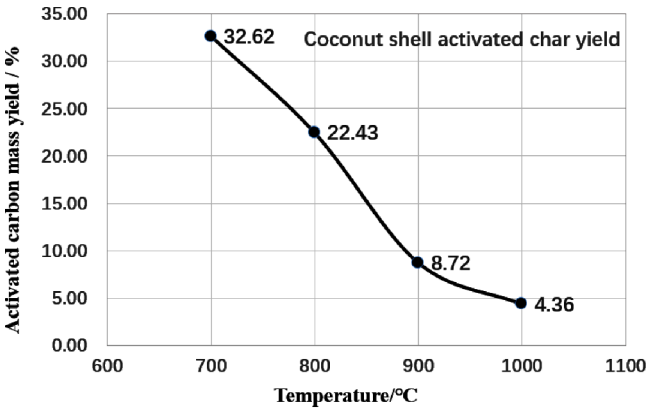

a) Activated carbon yield

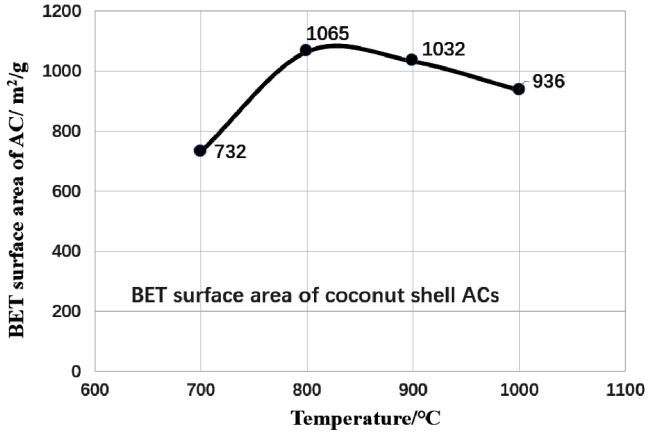

b) BET surface area of AC samples

Figure 3. Yield and BET surface area of activated carbon at different temperatures.

As shown in Figure 3, it can be seen that, with increasing activation temperature, the yield of activated carbon significantly declined. At 700 °C, the yield of coconut shell AC was about 32.62 wt %. However, the BET specific surface area was 732 m^2/g. It means that the activation reaction did not fully take place. Therefore, fewer pores were produced. When the activation temperature increased to 800 °C, the yield of AC decreased to 22.43 wt %, while the BET specific surface area increased to 1065 m^2/g. Higher temperature benefits the char−steam reaction. The detailed activation reactions are summarized in Table 2.

Table 2. Main Gasification Reactions during Char−Steam Activation

Reaction[39−41]	Enthalpy (kJ/mol)[39−41]
$C + H_2O \rightarrow CO + H_2$ (R1)	$\Delta H = -135.0$
$C + CO_2 \rightarrow 2CO$ (R2)	$\Delta H = -173.3$
$CO + H_2O \rightleftharpoons CO_2 + H_2$ (R3)	$\Delta H = 41.0$
$C + 2H_2 \rightarrow CH_4$ (R4)	$\Delta H = 84.3$
$CH_4 + H_2O \rightleftharpoons CO + 3H_2$ (R5)	$\Delta H = -21.9$

As show in Table 2, during steam activation, char gasification (R1) is the dominant reaction, which is an endothermal reaction.[42] It means that, when the temperature is improved, the reaction balance will move forward to produce more CO and H_2. The other reactions (R2−R5) are additional reactions that accompany the steam gasification process of biochar, which affected the final gas composition (CO, H_2, CO_2, CH_4, etc.) in the flue gas.

When the activation temperature increased to 900 °C, the AC yield quickly decreased to 8.72 wt %, while the BET surface area slightly declined to 1032 m^2/g. It means that high temperature could consume a lot of the carbon skeleton, resulting in the reduction of activated carbon yield. Therefore, selecting a reasonable temperature is one of the keys to the preparation of activated carbon. In this work, considering the yield and specific surface area of activated carbon, 800 °C was regarded as the optimized activation temperature for the coconut shell.

3.3. Chemical Activation of Lignin and Coconut Shell. Next, the chemical activation of lignin and coconut shell was conducted. KOH and K_2CO_3 were used as the activation agents, respectively. The activation results of K_2CO_3 activation are summarized in Figure 4.

Similar to steam activation, the yield of lignin AC decreased with increasing activation temperature. When the temperature increased from 500 to 800 °C, the yield of AC decreased from 62.72 to 25.38 wt % roughly linearly. With respect to BET specific surface area, the value first increased from 38.36 m^2/g (500 °C) to 1723.8 m^2/g (800 °C) and then slightly decreased to 1608.2 m^2/g. Improving activation enhanced the activation reaction and benefited the formation of micropores. With respect to the micropore and mesopore distribution, it can be seen that micropores contribute the majority of the specific surface area and the largest surface area of the micropores was about 1414.84 m^2/g. With increasing activation temperature, the micropores first increased and then declined, while the mesopores increased at all temperatures. It means that the overactivation reaction consumes micropores but promotes the formation of mesoporous cells. The variation of porosity with temperature is similar to the BET surface area. The largest porosity was about 0.951 at 800 °C. Considering the yield and specific surface area of activated carbon, 800 °C was regarded as the optimized activation temperature for lignin during K_2CO_3 activation. Mckee et al.[43] studied the gasification of graphite by alkali and found that K_2CO_3 reduced by carbon in graphite could be summarized as follows:

$$K_2CO_3 + 2C \rightarrow 2K + 3CO \quad \text{(R6)}$$

C represents the carbon element in biochar, which acts as the reducing agent and reduces K_2CO_3 to product metallic potassium and CO.

https://doi.org/10.1021/acsomega.4c00352
ACS Omega 2024, 9, 24453−24463

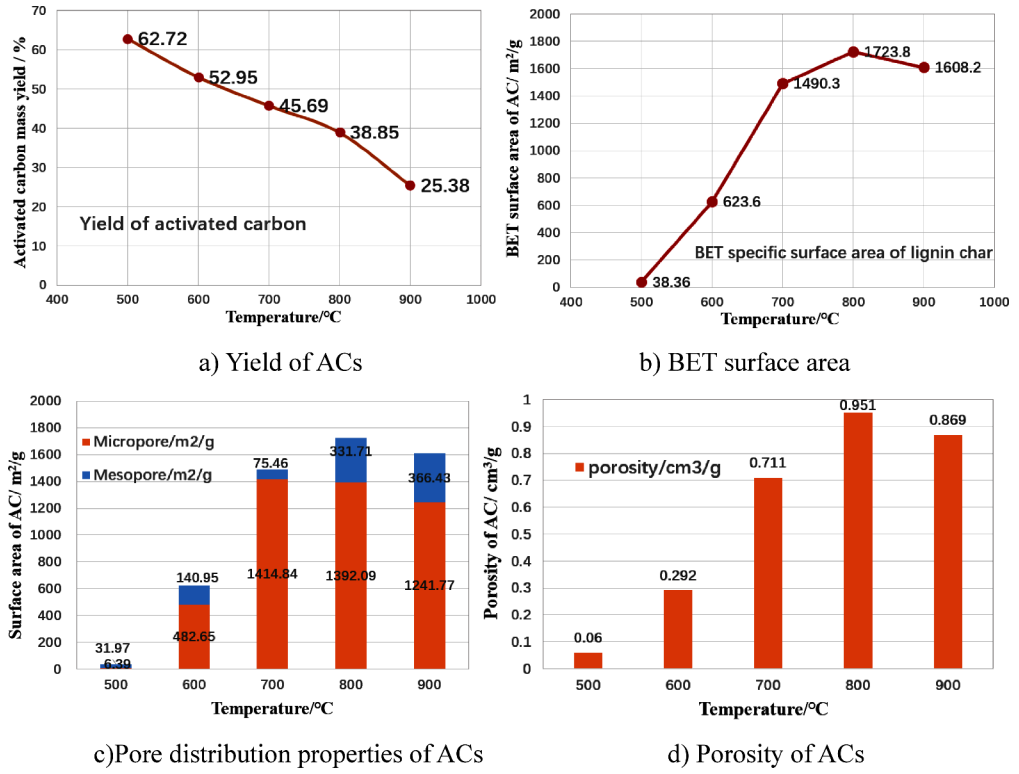

Figure 4. Lignin AC production by K_2CO_3 activation.

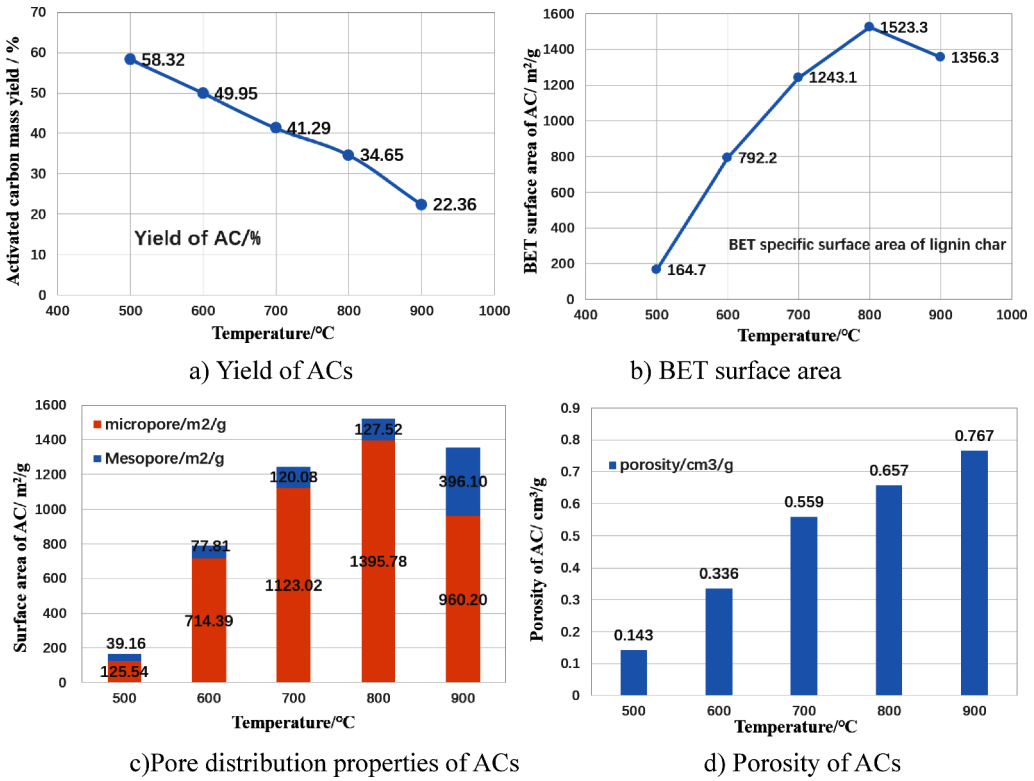

Figure 5. Lignin AC production by KOH activation.

As a contrast, KOH was used as an activator to study the chemical chemistry of lignin, and the results are shown in Figure 5.

The performance of the KOH activation was similar to that of K_2CO_3 activation. With the temperature increasing from 500 to 800 °C, the lignin AC yield decreased from 58.32 to 22.36 wt %. The BET surface area first increased with improving temperature and reached a maximum of 1523.3 m^2/g at 800 °C. With respect to the pore distribution, the variation tendency of micropore and mesopore is similar to that of lignin AC in K_2CO_3

https://doi.org/10.1021/acsomega.4c00352
ACS Omega 2024, 9, 24453−24463

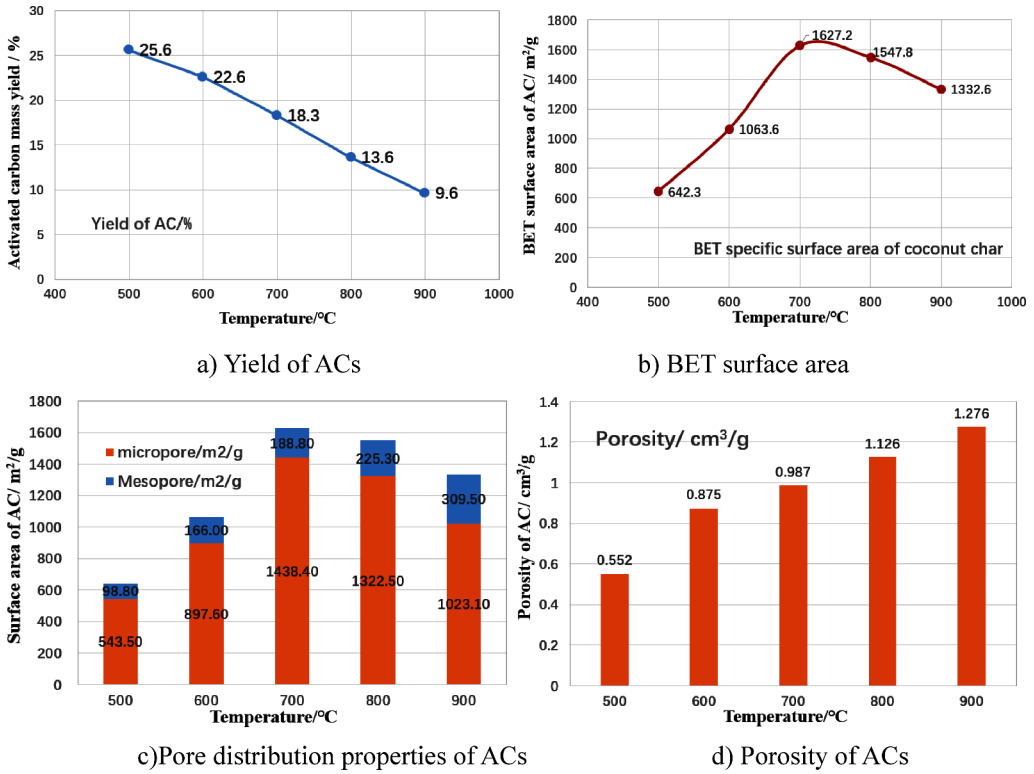

Figure 6. Coconut shell AC production by KOH activation.

activation. However, the porosity increased with an activation temperature even at 900 °C. It means that at high temperature, the KOH could enter the inside of the micropores, making the micropores expand, forming meso- and macroporous cells, and the overall coke skeleton structure is preserved. When lignin is activated by K_2CO_3, the activator easily causes the carbon skeleton to erode and the pore structure to collapse at high temperature, thus reducing the porosity. The possible reaction mechanisms are[44]

$$2KOH \rightarrow K_2O + H_2O \quad (R7)$$

$$2K_2O + 2C \rightarrow 4K + 2CO \quad (R8)$$

$$H_2O + C \rightarrow CO + H_2 \quad (R9)$$

It can be indicated that the K_2CO_3 activation could achieve higher AC yield as well as higher BET surface area for lignin. The porosity of K_2CO_3 activation of AC is significantly larger. Therefore, the lignin AC derived by K_2CO_3 activation was used for phenol adsorption in the next section.

As a comparison, the one-step activation of coconut shell by KOH was studied. Similarly, the influence of activation temperature on the yields, BET surface area, micropore/mesopore, and porosity of coconut shell AC was analyzed. The results are summarized in Figure 6.

It can be seen that the yield of coconut shell during KOH activation is much lower than that of lignin. When the activation temperature reaches 900 °C, the AC yield is about 9.6 wt %. The reason is that most cellulose and hemicellulose are largely consumed at higher temperature. Lignin is more stable than cellulose and lignin, which is attributed to its aromatic structure. With the increase of activation temperature, the BET surface area first increases and then decreases. The maximum of BET surface area is 1627.2 m^2/g at 700 °C, which is lower than that of lignin. The porosity of coconut shell AC is much larger than that of lignin AC, which is attributed to the consumption of cellulose and hemicellulose. More external pores, especially macropores, are produced. It can be indicated that the optimized activation temperature could be chosen as 700 °C for one step activation of the coconut shell by KOH.

In addition to the pore structure, the surface functional groups of activated carbon also have a key influence on its adsorption properties. Next, the FTIR spectrum results of different activated carbon samples are summarized in Figure 7.

It can be seen that the coconut shell raw material is rich in −OH, C−O, and C═O functional groups, which are the original components of cellulose, hemicellulose, and lignin. During activation, the −OH functional groups are largely consumed. With respect to the coconut shell AC samples, the C−O and C═O are the main oxygen-containing functional groups, which may act as the key adsorption site by electrostatic interaction. The FTIR spectrum results of lignin samples are different from those of the coconut shell. The spectral absorption intensity of −OH functional groups is much weaker than that of the coconut shell. The reason is that cellulose and hemicellulose have more −OH functional groups than does lignin. With respect to the lignin AC samples, the −OH functional groups are almost consumed. The C−O and C═O are main oxygen-containing functional groups. Especially for lignin AC derived by K_2CO_3 activation, the −C−O group is much more than other functional groups. It means that K_2CO_3 activation could largely enhance the formation of surface oxygen-containing functional groups.

3.4. Adsorption of Phenol by Activated Carbon. Figure 8 shows the effects of the activation temperature and adsorption time on the adsorption performance of coconut shell AC and lignin AC for phenol. With respect to coconut shell, three kinds of steam activation coconut shell AC samples and KOH activation AC sample (700 °C) were used. Besides, two kinds of

https://doi.org/10.1021/acsomega.4c00352
ACS Omega 2024, 9, 24453−24463

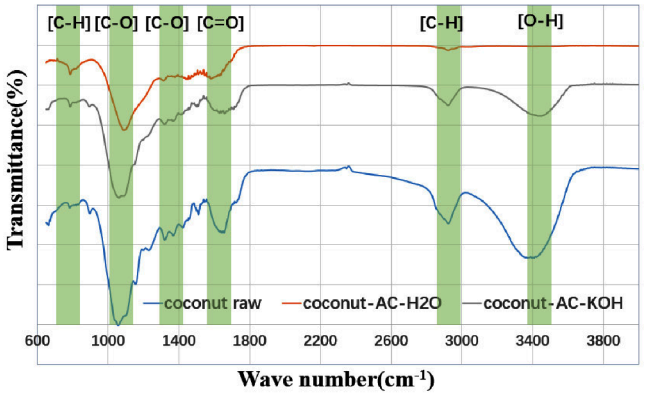

(a) FTIR curves of coconut shell samples

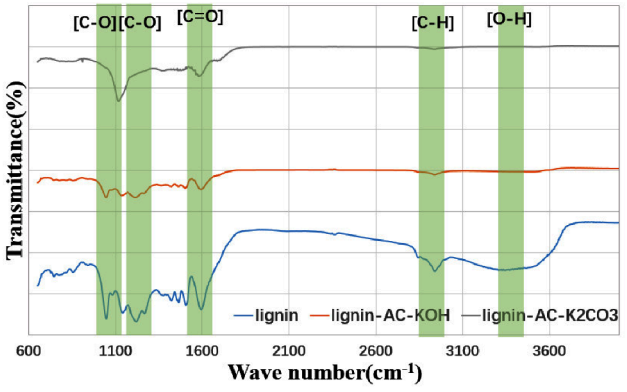

(b) FTIR curves of lignin samples

Figure 7. FTIR results of coconut shell and lignin samples.

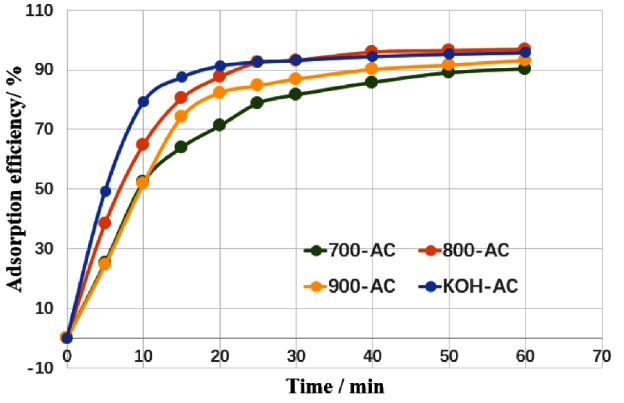

(a) Coconut shell AC samples

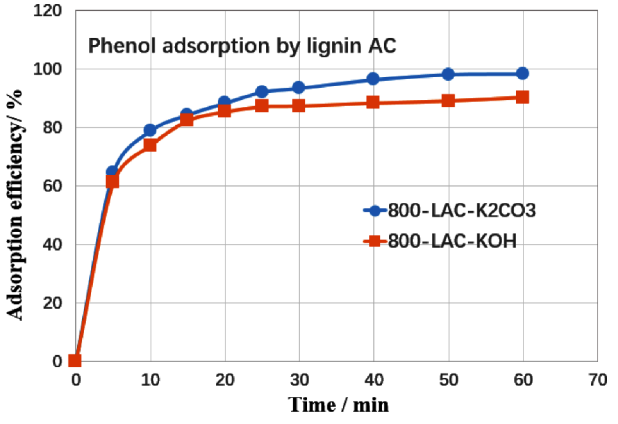

(b) Lignin AC samples

Figure 8. Effect of time on the phenol adsorption by coconut shell AC and lignin AC.

lignin AC samples were used, including K_2CO_3 activation at 800 °C and KOH activation at 800 °C. The adsorption time is from 0 to 60 min. For each adsorption experiment, 50 mL of phenol solution was placed in a brown reagent bottle, and 0.1 g of adsorbent (activated carbon) was added into the phenol solution. Then the concentration of phenol in the solution was determined after stirring at 30 °C for a certain time. The adsorption efficiency of phenol was obtained by the concentration difference.

It can be seen from Figure 8 that the adsorption rate of all activated carbon samples increases sharply at first 10 min, then slowly increases at 20−30 min, and finally tends toward a stable value. After 40 min of adsorption, the adsorption of the three samples basically reached equilibrium, and the adsorption efficiency did not change significantly. Comparing different coconut shell activated carbon, it can be seen that the 800 °C activated coconut shell activated carbon has the highest adsorption efficiency, and its stable adsorption efficiency at 60 min is about 96.87%. Based on the porosity of the coconut shell AC samples, the BET surface area of coconut shell AC derived at 800 °C was the largest. It can be indicated that the BET surface area largely influenced the phenol adsorption efficiency. Better porosity and larger specific surface area can provide more transport channels and a larger attachment area for phenol molecules, so more phenol molecules can be adsorbed in a shorter time. Therefore, improving the specific surface area of coconut shell activated carbon is one of the key points. Compared with steam activation, the KOH activation AC shows better performance in the first 20 min. Especially at initial 10 min, phenol is quickly adsorbed by coconut shell AC. Coconut shell AC derived by KOH activation has larger porosity and BET surface area. Besides, the chemical activation may introduce more active functional groups on the char surface, which could enhance the adsorption ability for phenol.

The adsorption properties of lignin activated carbon for phenol are similar to those of coconut shell activated carbon. At the initial stage (0−5 min), the amount of adsorption increases rapidly, then increases slowly (5−30 min), and then remains at a stable level (after 30 min). Compared with coconut shell ACs, the adsorption rate of phenol by lignin AC is faster, and the adsorption capacity is stronger. The largest phenol adsorption efficiency at 60 min for 800-LAC-K_2CO_3 is about 98.22%, which is much higher than that for coconut shell ACs. Besides, 800-LAC-K_2CO_3 shows better performance than 800-LAC-KOH. As pointed out above, the adsorption performance largely depends on the physical porosity structure. K_2CO_3 activation lignin AC at 800 °C has the largest BET specific area (1723.8 m^2/g) of all AC samples and shows the best phenol adsorption performance (98.22%).

Next, the effect of adsorption temperature (20−60 °C) on phenol adsorption by coconut shell AC and lignin AC samples is shown in Figure 9.

As can be seen from Figure 9(a), the adsorption rate gradually decreases with the increase in adsorption temperature. At 20 °C, the adsorption rate was 96.87%. When the adsorption temperature rises to 60 °C, the adsorption rate decreases to 92.35%. With the increase of temperature, although the movement speed of phenol molecules increases, it is easy to

https://doi.org/10.1021/acsomega.4c00352
ACS Omega 2024, 9, 24453−24463

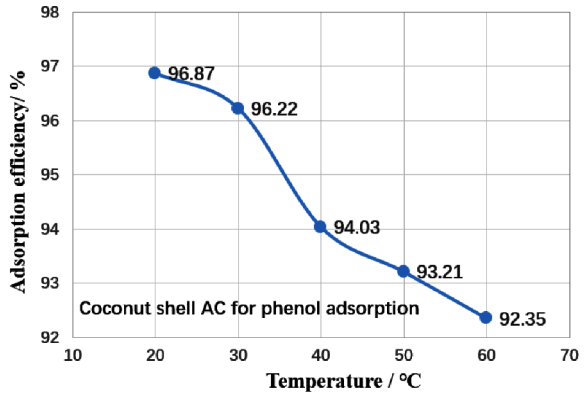

(a) Coconut shell AC

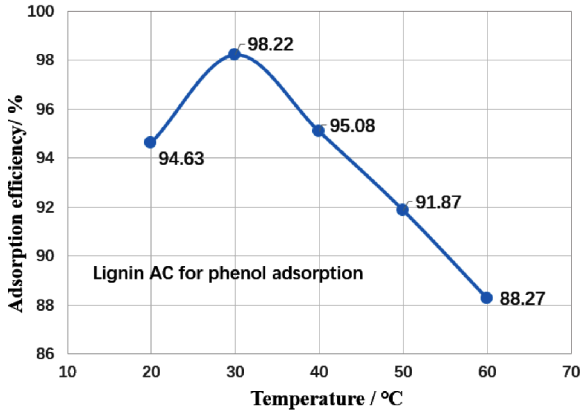

(b) Lignin AC

Figure 9. Effect of temperature on the phenol adsorption by coconut shell AC and lignin AC.

enter the pore interior, but the higher temperature also promotes the adsorbed phenol molecules to fall off more easily, that is, desorption. The increase of temperature destroyed the dynamic equilibrium of the solution and promoted the desorption of more phenol molecules, so the adsorption amount decreased with the increase of temperature.

As can be seen from Figure 9(b), the adsorption efficiency of lignin activated carbon for phenol first increased and then decreased with the increased adsorption temperature, and reached the maximum value (98.22%) at 30 °C. When the temperature increased from 20 to 30 °C, the adsorption efficiency increased. When the adsorption temperature further increased to 60 °C, the adsorption efficiency gradually decreased to 88.27%. As mentioned above, increasing the adsorption temperature changes the adsorption equilibrium of phenol molecules on the surface of activated carbon and the equilibrium moves toward desorption. With the rapid adsorption of phenol molecules, more phenol molecules were desorbed from the AC surface. Therefore, 30 °C is an optimized adsorption temperature for phenol removal over lignin AC.

In summary, the adsorption effect of K_2CO_3 activated lignin AC for phenol is better than that of KOH activated carbon, and the lignin activated carbon has a stronger adsorption performance for phenol than coconut shell activated carbon. According to the pore structure characteristics, it can be preliminarily concluded that developed micropores are the main sites for phenol adsorption, while mesopores and macropores are the main channels for phenol molecular transport. The role of mesopores and macropores on transport have been widely studied.[45,46] The well-developed microscopic pores and reasonable pore distribution are important parameters to ensure the adsorption and removal efficiency of phenol by activated carbon. Besides, as discussed above, the abundant oxygen-containing functional groups during K_2CO_3 activation could largely provide more active sites on the char surface and enhance the adsorption performance for phenol.

3.5. Kinetic Analysis of the Phenol Adsorption on AC Samples. According to the type of adsorption isotherm, the surface properties of the adsorbent and the interaction between the adsorbent and adsorbent can be known. The kinetic analysis of the phenol adsorption on different activated carbon samples provided some information about the interaction between activated carbon and phenol molecules. In addition, the kinetic parameters could be used for the design and operation optimization of phenol removal by activated carbons. In this section, based on the phenol adsorption experiments, the adsorption kinetic analysis was conducted. The pseudo-first-order kinetic model was used to describe the adsorption process. The following equation can be obtained by taking the logarithmic deformation of both sides for eq 2 in section 2.2.

$$\ln\left(1 - \frac{Q_t}{Q_e}\right) = -kt \tag{3}$$

Using eq 3, the linear relation between $\ln(1 - Q_t/Q_e)$ and t could be plotted, and the kinetic constant k could be obtained. The linear regression of the phenol adsorption by coconut shell AC samples is summarized in Figure 10.

It can be indicated that the mean square errors (MSE) of linear regression are 0.9714, 0.9652, and 0.9192, respectively, for steam activation samples. The pseudo-first-order kinetic model is able to describe the adsorption characteristics of phenol in coconut shell activated carbon. The adsorption rate constants for three AC samples are 0.0551, 0.0915, and 0.0716, respectively, which indicated that coconut shell AC derived at 800 °C shows the best adsorption performance for phenol adsorption. With respect to the KOH activation sample, the MSE and adsorption rate constant are 0.8477 and 0.0772.

Similarly, the linear regression of the phenol adsorption by lignin ACs is analyzed, and the results are summarized in Figure 11.

It can be seen from Figure 11 that the pseudo-first-order kinetic model is able to describe the adsorption characteristics of phenol in lignin activated carbon, especially for KOH activation samples. The adsorption rate constants are 0.06621 and 0.04496, respectively, which indicated that the lignin AC activated by K_2CO_3 has a stronger adsorption capacity for phenol.

3.6. Recycling and Regeneration Characteristic for Phenol Adsorption. In this section, the recycling characteristics of adsorption of phenol by lignin activated carbon were studied. The used lignin activated carbon adsorbent was recovered and soaked in methanol for 2 h and then dried in an oven at 60 °C for 24 h for the next adsorption. The adsorption performance after cycles is summarized in Figure 12.

It can be seen from Figure 12 that, after three cycles, the adsorption rate of lignin activated carbon can still remain higher than 93%, showing high adsorption performance. It can be inferred that, after more cycles, the adsorption performance of activated carbon will further decrease to even lower than 90%.

https://doi.org/10.1021/acsomega.4c00352
ACS Omega 2024, 9, 24453−24463

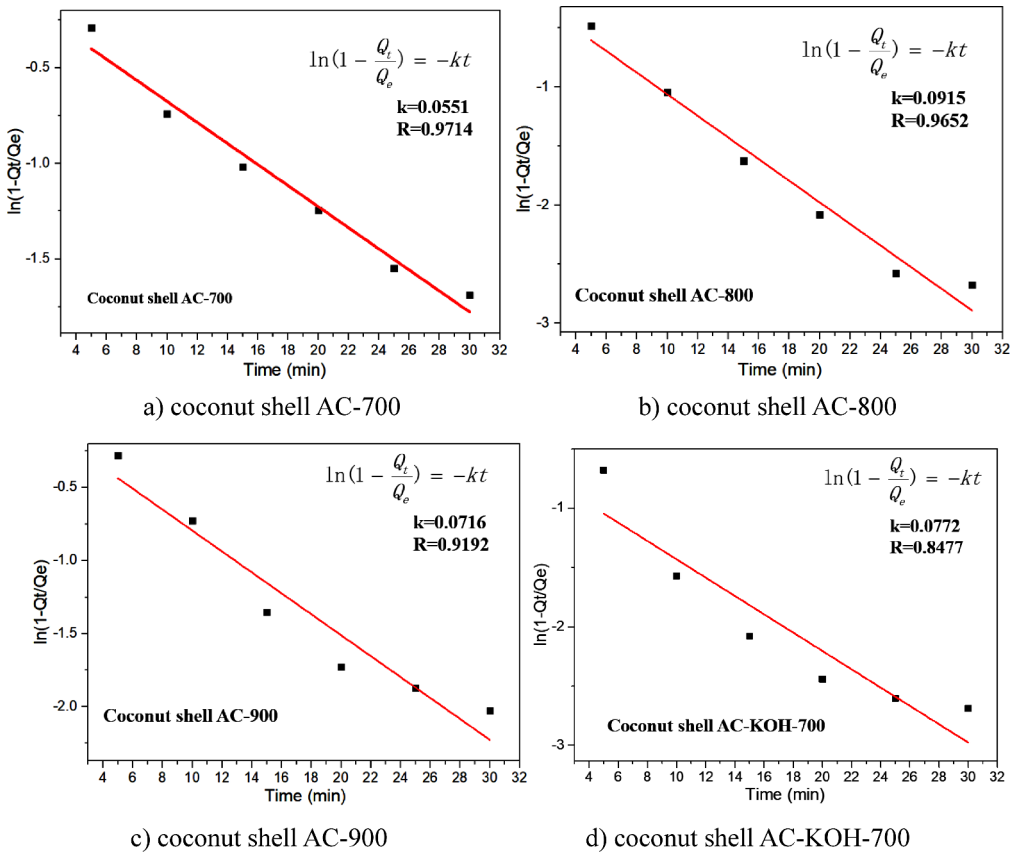

Figure 10. Linear regression of the phenol adsorption by coconut shell ACs.

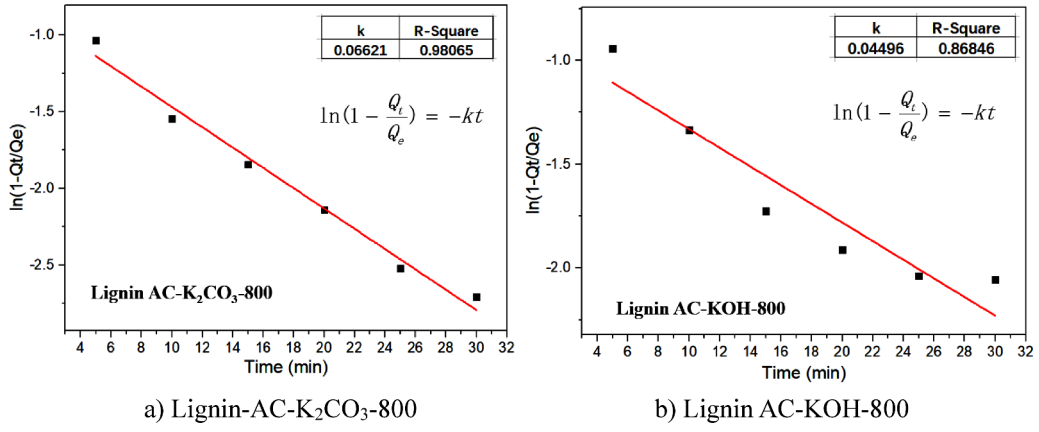

Figure 11. Linear regression of the phenol adsorption by lignin ACs.

Regardless, these results confirmed that the lignin activated carbon had a good adsorption stability.

4. CONCLUSION

Biomass waste and sewage are important wastes in the process of industrialization and need to be effectively disposed and utilized. In this work, an innovative method of collaborative treatment of biomass waste and phenol-containing wastewater is proposed. Biomass waste was used to produce activated carbon (AC) and then AC was used for phenol removal in sewage treatment. Two kinds of typical biomass waste material, namely, coconut shell and lignin were used. Physical activation (steam activation) and chemical activation methods were compared. The main conclusion could be summarized as follows:

The optimized pyrolysis temperature could be chosen as 500 °C for initial char production. Steam activation is an effective method for coconut shell AC production. The largest BET surface area was 1065 m^2/g at 800 °C. Chemical activation could produce AC samples with higher BET specific surface area. The lignin AC with K_2CO_3 activation has the largest BET surface of 1723.8 m^2/g at 800 °C, which is higher than that with KOH activation (1523.3 m^2/g). FTIR results indicated that K_2CO_3 activation could largely enhance the formation of surface oxygen-containing functional groups.

Both coconut shell AC and lignin AC samples show excellent performance for phenol removal. The highest phenol removal efficiency for coconut shell AC and lignin AC are 96.87% and 98.22%, respectively. Adsorption kinetic analysis shows that the

https://doi.org/10.1021/acsomega.4c00352
ACS Omega 2024, 9, 24453−24463

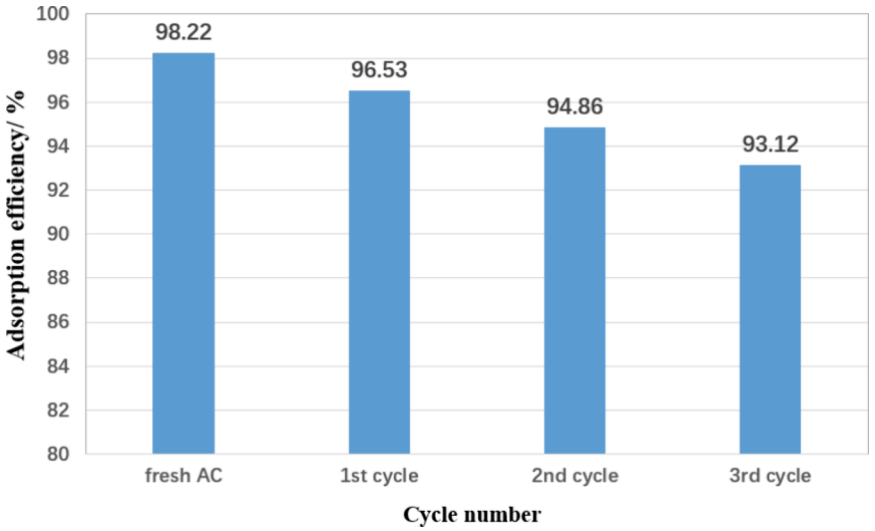

Figure 12. Recycling characteristic of phenol adsorption.

pseudo-first-order kinetic model is able to describe the adsorption characteristics of phenol in sewage treatment. Recycling properties show that regeneration of lignin AC could maintain high adsorption performance for phenol.

This work provides a new approach for the collaborative treatment of biomass waste and phenol-containing sewage.

AUTHOR INFORMATION

Corresponding Author

Yuting Li − *School of Chemistry and Environmental Engineering, Shanghai Institute of Technology, Shanghai 201418, China;* orcid.org/0009-0005-0942-6256; Email: l346215426@163.com

Authors

Ping Cao − *School of Chemistry and Environmental Engineering, Shanghai Institute of Technology, Shanghai 201418, China*

Jingli Shao − *Shanghai Composite Material Science & Technology Co., Ltd., Shanghai 201112, China*

Complete contact information is available at: https://pubs.acs.org/10.1021/acsomega.4c00352

Notes

The authors declare no competing financial interest.

ACKNOWLEDGMENTS

There is no applicable funding.

REFERENCES

(1) Wang, K.; Zhuang, T.; Su, Z.; Chi, M.; Wang, H. Antibiotic residues in wastewaters from sewage treatment plants and pharmaceutical industries: Occurrence, removal and environmental impacts. *Science of The Total Environment* **2021**, *788*, 147811.

(2) Douara, N.; Bestani, B.; Benderdouche, N.; Duclaux, L. Sawdust-based activated carbon ability in the removal of phenol-based organics from aqueous media. *Desalination and Water Treatment* **2016**, *57* (12), 5529−5545.

(3) Wang, L.; Chang, Y.; Zhang, X.; Yang, F.; Li, Y.; Yang, X.; Dong, S. Hydrothermal co-carbonization of sewage sludge and high concentration phenolic wastewater for production of solid biofuel with increased calorific value. *Journal of Cleaner Production* **2020**, *255*, 120317.

(4) Mohamad Said, K. A.; Ismail, A. F.; Abdul Karim, Z.; Abdullah, M. S.; Hafeez, A. A review of technologies for the phenolic compounds recovery and phenol removal from wastewater. *Process Safety and Environmental Protection* **2021**, *151*, 257−289.

(5) Saha, N.; Bhunia, F.; Kaviraj, A. Toxicity of phenol to fish and aquatic ecosystems. *Bull. Environ. Contam. Toxicol.* **1999**, *63*, 195−202.

(6) Mohamad Said, K. A.; Ismail, A. F.; Abdul Karim, Z.; Abdullah, M. S.; Hafeez, A. A review of technologies for the phenolic compounds recovery and phenol removal from wastewater. *Process Safety and Environmental Protection* **2021**, *151*, 257−289.

(7) Grace Pavithra, K.; Sundar Rajan, P.; Arun, J.; Brindhadevi, K.; Hoang Le, Q.; Pugazhendhi, A. A review on recent advancements in extraction, removal and recovery of phenols from phenolic wastewater: Challenges and future outlook. *Environmental Research* **2023**, *237*, 117005.

(8) Eryılmaz, C.; Genc, A. Review of Treatment Technologies for the Removal of Phenol from Wastewaters. *Journal of Water Chemistry and Technology* **2021**, *43* (2), 145−154.

(9) Cifuentes-Cabezas, M.; María Sanchez-Arévalo, C.; Antonio Mendoza-Roca, J.; Cinta Vincent-Vela, M.; Álvarez-Blanco, S. Recovery of phenolic compounds from olive oil washing wastewater by adsorption/desorption process. *Sep. Purif. Technol.* **2022**, *298*, 121562.

(10) Stavropoulos, G. G.; Samaras, P.; Sakellaropoulos, G. P. Effect of activated carbons modification on porosity, surface structure and phenol adsorption. *Journal of Hazardous Materials* **2008**, *151* (2), 414−421.

(11) Carrasco, J.; Klimeš, J.; Michaelides, A. The role of van der Waals forces in water adsorption on metals. *J. Chem. Phys.* **2013**, *138* (2), 024708.

(12) Peng, Y.; Wei, X.; Wang, Y.; Li, W.; Zhang, S.; Jin, J. Metal-organic framework composite photothermal membrane for removal of high-concentration volatile organic compounds from water via molecular sieving. *ACS Nano* **2022**, *16* (5), 8329−8337.

(13) Velusamy, S.; Roy, A.; Sundaram, S.; Kumar Mallick, T. A review on heavy metal ions and containing dyes removal through graphene oxide-based adsorption strategies for textile wastewater treatment. *Chem. Rec.* **2021**, *21* (7), 1570−1610.

(14) Ahmad, A. A.; Hameed, B. H. Reduction of COD and color of dyeing effluent from a cotton textile mill by adsorption onto bamboo-based activated carbon. *Journal of Hazardous Materials* **2009**, *172* (2), 1538−1543.

(15) Patel, P.; Muteen, A.; Mondal, P. Treatment of greywater using waste biomass derived activated carbons and integrated sand column. *Science of The Total Environment* **2020**, *711*, 134586.

https://doi.org/10.1021/acsomega.4c00352
ACS Omega 2024, 9, 24453−24463

(16) Ferraz, F. M.; Yuan, Q. Performance of oat hulls activated carbon for COD and color removal from landfill leachate. *Journal of Water Process Engineering* **2020**, *33*, 101040.
(17) Khurshid, H.; Mustafa, M. R. U.; Rashid, U.; Isa, M. H.; Ho, Y. C.; Shah, M. M. Adsorptive removal of COD from produced water using tea waste biochar. *Environmental Technology & Innovation* **2021**, *23*, 101563.
(18) Hassan, M. M.; Carr, C. M. Biomass-derived porous carbonaceous materials and their composites as adsorbents for cationic and anionic dyes: A review. *Chemosphere* **2021**, *265*, 129087.
(19) Oyekunle, D. T.; Zhou, X.; Shahzad, A.; Chen, Z. Review on carbonaceous materials as persulfate activators: structure-performance relationship, mechanism and future perspectives on water treatment. *Journal of Materials Chemistry A* **2021**, *9* (13), 8012−8050.
(20) Hong, D.; Zhou, J.; Hu, C.; Zhou, Q.; Mao, J.; Qin, Q. Mercury removal mechanism of AC prepared by one-step activation with ZnCl2. *Fuel* **2019**, *235*, 326−335.
(21) Mohd Din, A. T.; Hameed, B. H.; Ahmad, A. L. Batch adsorption of phenol onto physiochemical-activated coconut shell. *Journal of Hazardous Materials* **2009**, *161* (2), 1522−1529.
(22) Deng, Z.; Sun, S.; Li, H.; Pan, D.; Patil, R. R.; Guo, Z.; Seok, I. Modification of coconut shell-based activated carbon and purification of wastewater. *Advanced Composites and Hybrid Materials* **2021**, *4*, 65−73.
(23) Ralph, J.; Lapierre, C.; Boerjan, W. Lignin structure and its engineering. *Curr. Opin. Biotechnol.* **2019**, *56*, 240−249.
(24) Arkell, A.; Olsson, J.; Wallberg, O. Process performance in lignin separation from softwood black liquor by membrane filtration. *Chem. Eng. Res. Des.* **2014**, *92* (9), 1792−1800.
(25) Dieste, A. s.; Clavijo, L.; Torres, A. I.; Barbe, S. p.; Oyarbide, I.; Bruno, L.; Cassella, F. Lignin from Eucalyptus spp. kraft black liquor as biofuel. *Energy Fuels* **2016**, *30* (12), 10494−10498.
(26) Fu, K.; Yue, Q.; Gao, B.; Sun, Y.; Zhu, L. Preparation, characterization and application of lignin-based activated carbon from black liquor lignin by steam activation. *Chemical Engineering Journal* **2013**, *228*, 1074−1082.
(27) Zhao, J.; Zhang, W.; Shen, D.; Zhang, H.; Wang, Z. Preparation of porous carbon materials from black liquor lignin and its utilization as CO2 adsorbents. *Journal of the Energy Institute* **2023**, *107*, 101179.
(28) Revellame, E. D.; Fortela, D. L.; Sharp, W.; Hernandez, R.; Zappi, M. E. Adsorption kinetic modeling using pseudo-first order and pseudo-second order rate laws: A review. *Cleaner Engineering and Technology* **2020**, *1*, 100032.
(29) Simonin, J.-P. On the comparison of pseudo-first order and pseudo-second order rate laws in the modeling of adsorption kinetics. *Chemical Engineering Journal* **2016**, *300*, 254−263.
(30) Naderi, M. Chapter Fourteen - Surface Area: Brunauer-Emmett-Teller (BET). In *Progress in Filtration and Separation*; Tarleton, S., Ed.; Academic Press: Oxford, 2015; pp 585−608.
(31) Pickett, G. Modification of the Brunauer—Emmett—Teller theory of multimolecular adsorption. *J. Am. Chem. Soc.* **1945**, *67* (11), 1958−1962.
(32) Wang, G.; Wang, K.; Ren, T. Improved analytic methods for coal surface area and pore size distribution determination using 77K nitrogen adsorption experiment. *International Journal of Mining Science and Technology* **2014**, *24* (3), 329−334.
(33) Pasangulapati, V.; Ramachandriya, K. D.; Kumar, A.; Wilkins, M. R.; Jones, C. L.; Huhnke, R. L. Effects of cellulose, hemicellulose and lignin on thermochemical conversion characteristics of the selected biomass. *Bioresour. Technol.* **2012**, *114*, 663−669.
(34) Yang, H.; Yan, R.; Chen, H.; Lee, D. H.; Zheng, C. Characteristics of hemicellulose, cellulose and lignin pyrolysis. *Fuel* **2007**, *86* (12), 1781−1788.
(35) Stefanidis, S. D.; Kalogiannis, K. G.; Iliopoulou, E. F.; Michailof, C. M.; Pilavachi, P. A.; Lappas, A. A. A study of lignocellulosic biomass pyrolysis via the pyrolysis of cellulose, hemicellulose and lignin. *Journal of Analytical and Applied Pyrolysis* **2014**, *105*, 143−150.
(36) Wei, X.; Li, T. Wooden activated carbon production for dioxin removal via a two-step process of carbonization coupled with steam activation from biomass wastes. *ACS omega* **2021**, *6* (8), 5607−5618.
(37) Sekine, Y.; Ishikawa, K.; Kikuchi, E.; Matsukata, M.; Akimoto, A. Reactivity and structural change of coal char during steam gasification. *Fuel* **2006**, *85* (2), 122−126.
(38) Zhai, M.; Xu, Y.; Guo, L.; Zhang, Y.; Dong, P.; Huang, Y. Characteristics of pore structure of rice husk char during high-temperature steam gasification. *Fuel* **2016**, *185*, 622−629.
(39) Dhanavath, K. N.; Shah, K.; Bhargava, S. K.; Bankupalli, S.; Parthasarathy, R. Oxygen-steam gasification of karanja press seed cake: Fixed bed experiments, ASPEN Plus process model development and benchmarking with saw dust, rice husk and sunflower husk. *Journal of Environmental Chemical Engineering* **2018**, *6* (2), 3061−3069.
(40) Puig-Gamero, M.; Argudo-Santamaria, J.; Valverde, J.; Sánchez, P.; Sanchez-Silva, L. Three integrated process simulation using aspen plus®: Pine gasification, syngas cleaning and methanol synthesis. *Energy conversion and management* **2018**, *177*, 416−427.
(41) Cao, Y.; Wang, Q.; Du, J.; Chen, J. Oxygen-enriched air gasification of biomass materials for high-quality syngas production. *Energy conversion and management* **2019**, *199*, 111628.
(42) Shang, Z.; Yang, Z.; Ma, Y. Theoretical study of activated carbon production via a two-step carbonization-activation process based on Aspen Plus calculation. *Biomass Conversion and Biorefinery* **2023**, *13* (9), 8267−8276.
(43) McKee, D. W. Mechanisms of the alkali metal catalysed gasification of carbon. *Fuel* **1983**, *62* (2), 170−175.
(44) Mariana, M.; Mistar, E. M.; Alfatah, T.; Supardan, M. D. High-porous activated carbon derived from Myristica fragrans shell using one-step KOH activation for methylene blue adsorption. *Bioresource Technology Reports* **2021**, *16*, 100845.
(45) Tallarek, U.; Hlushkou, D.; Höltzel, A. Solute sorption, diffusion, and advection in macro-mesoporous materials: Toward a realistic bottom-up simulation strategy. *J. Phys. Chem. C* **2022**, *126* (5), 2336−2348.
(46) Fang, B.; Kim, J. H.; Kim, M.-S.; Yu, J.-S. Hierarchical nanostructured carbons with meso-macroporosity: design, characterization, and applications. *Acc. Chem. Res.* **2013**, *46* (7), 1397−1406.

https://doi.org/10.1021/acsomega.4c00352
ACS Omega 2024, 9, 24453−24463